Journal of Applied Microbiology, 2025, 136(10), lxaf247
https://doi.org/10.1093/jambio/lxaf247
Advance access publication date: 6 October 2025
Research Article

JOURNAL OF
APPLIED
MICROBIOLOGY
OXFORD
UNIVERSITY PRESS

Candidate biomarkers of lead-exposed municipal water biofilms provide insights into lead monitoring potential

Nahreen Mirza[1], **Md Hadiuzzaman**[2], **David A. Ladner**[3], **Maryam Salehi**[4,5], **Shawn P. Brown**[1,6,*]

[1]Department of Biological Sciences, The University of Memphis, Memphis, TN 38152, USA
[2]Illinois Sustainable Technology Center, University of Illinois at Urbana-Champaign, Champaign, IL 61801, USA
[3]Department of Environmental Engineering and Earth Sciences, Clemson University, Anderson, SC 29634, USA
[4]Department of Civil and Environmental Engineering, University of Missouri, Columbia, MO 65211, USA
[5]Missouri Water Center, University of Missouri, Columbia, MO 65211, USA
[6]Institute of Agricultural and Conservation Research and Education, The University of Memphis, Memphis, TN 38152, USA
*Corresponding author. Department of Biological Sciences, The University of Memphis, Memphis, TN 38152 USA. E-mail: spbrown2@memphis.edu

Abstract

Aims: Premise plumbing systems are prone to biofilm development, and depending on municipal water source and infrastructure, may be susceptible to heavy metal exposure, including lead (Pb). We aimed to investigate the impacts of Pb on municipal water biofilms and to elucidate the interactive effects of time, pipe material, and Pb concentration of biofilms. Further, we aimed to understand if after a Pb-exposure event, microbial biomarkers indicative of previous Pb exposure may remain, which may assist public health and water regulatory agencies in triaging human health concerns postexposure.

Methods and Results: We developed biofilms within pipe loops constructed from both cross-linked polyethylene (PEX-A) and high-density polyethylene (HDPE) plastics and exposed them to different concentrations of Pb (0, 5, and 500 $\mu g\ l^{-1}$) for 4 and 8 weeks, followed by 4 weeks of exposure to lead-free water to examine community shifts following a lead exposure event. Using bacterial metabarcoding and biomarker analyses, we show that Pb exposure shifts community structure and we identified several key taxa associated with lead exposure events and demonstrate that these taxa persist even after lead is removed from the system.

Conclusions: Taken together, this work provides a framework for identifying past Pb-exposure events that can be used for precautionary monitoring for human Pb exposures.

Impact Statement

Lead exposure leads to significant and long-lasting changes in bacterial biofilm communities in municipal plumbing pipes. These changes persist even after lead is removed from the system, and these changes may be diagnostic of lead exposure events. This provides a framework for using molecular microbial biomarkers to identify previously undetected municipal lead exposure events to assist public health triage.

Keywords: biofilms; amplicon sequencing; applied microbiology; drinking water; microbial community

Introduction

Municipal drinking water quality can have major impacts on public health, the economy, and environmental sustainability. In the United States, it is mandated by the National Primary Drinking Water Regulations (NPDWRs; enforced by the US Environmental Protection Agency) that public water systems must be below defined contaminant thresholds with an US Environmental Protection Agency (EPA) action level of 15 ppb of lead. However, rarely are lead concentrations measured from within premise plumbing, and once water is routed into a household or business main water line, water quality can deteriorate rapidly (Tsaridou and Karabelas 2021).

One of the main causes of poor household water quality is insufficient levels or degraded disinfectant residuals, high surface-to-volume ratio of pipes, and/or extended stagnation/retention duration, which may favor microbiological growth (Wang et al. 2013). The National Academies of Sciences and Medicine (2020) reported that there are at least 1.6 million kilometers of distribution mains and >9.7 million kilometers of premise plumbing within the United States. This increases the probability of even rare opportunistic pathogenic microorganisms flourishing within premises plumbing (Feazel et al. 2009). Additionally, it has been suggested pipe material, disinfectants type, water age, and water temperature can all impact microorganisms found within plumbing systems (Wang et al. 2012, Buse et al. 2014, Proctor et al. 2017, Neu and Hammes 2020). Furthermore, studies have demonstrated that plumbing stagnation of water within plumbing systems can result in a significant reduction of disinfectant residuals, an increase in microbial cell count, the growth of opportunistic pathogens, and changes in bacterial communities (Lautenschlager et al. 2010, Ling et al. 2018, Montagnino et al. 2022). To complicate microbiological concerns, most microorganisms within premise plumbing are found within biofilms, which are communities of microorganisms attached to the inner surface of the pipe encased in a matrix of extracellular polymeric substances (EPS), which reduces disinfectant efficacy (Lee et al. 2021). Coupled with microbiological concerns, a major concern associated with water quality is the presence of heavy metals, predominantly lead (Pb). Lead contamination in drinking water may occur due to changes in water chemistry, after long-term stagnation,

Received 31 May 2025; **revised** 18 September 2025; **accepted** 20 September 2025

or can be leached from fixtures and/or soldering (Rosen et al. 2017, Ghoochani et al. 2023). Within premise plumbing often has varied usage patterns and may be subjected to extended periods of stagnation during technical maintenance and vacations (Council 2010, Viglione 2020, Salehi et al. 2021). Because of this, premise plumbing might be more susceptible than other drinking water distribution system components to biofilm detachment and/or heavy metal contamination, scale resuspension, and the harmful effects on water quality and human health that result from these events.

Despite strict regulations about water quality in the US, drinking water is not free of microorganisms. These microbes can colonize inner surfaces of plumbing pipes and form biofilms (Ahamed et al. 2020, Ghoochani et al. 2023) and the level of colonization is determined by many factors, including pipe material (Hadiuzzaman et al. 2023), flow conditions, water chemistry, and temperature (Ibekwe and Murinda 2019, Calero Preciado et al. 2022), among others. Consequently, there is a movement to decrease reliance on metallic pipes in favor of plastic pipes in distribution and plumbing systems as they are often viewed as "cleaner" alternatives (Kim and Herrera 2010). However, this transition to plastic plumbing may exacerbate water quality concerns. Generally, bacterial communities that form biofilms are structured by the diversity of the organic materials available in the surrounding environment (Raghupathi et al. 2017), and leachates from these plastic pipes may stimulate microbial activity and growth (Romera-Castillo et al. 2018, Egea et al. 2024). For most pipes, about 90% of the total microbial biomass remains embedded within the matrix attached to the pipe walls and the rest disperses into the encircling water (Flemming et al. 2002). Despite the concerns of microbiological and heavy metal contamination, the interactions between biofilms and heavy metals within plastic potable water pipes are poorly studied. Recent work has indicated that biofilms on plastic plumbing pipe surfaces increases the affinity of heavy metal adsorption and facilitates release back into the water, depending on physicochemical or water flow conditions (Ghoochani et al. 2023, Hadiuzzaman et al. 2023).

Many lead-resistant bacteria, which may be common in drinking water (Calomiris et al. 1984), survive potential lead toxicity using metallothioneins (MTs). MTs are proteins that bind to metals and are found in many bacterial taxa and their distribution is controlled by ecological influences and evolutionary pressures (Blindauer et al. 2002). To protect enzyme-catalyzed bacterial metabolic activities, heavy metals are immobilized by MTs (Nong et al. 2019), which can result in sequestration of heavy metals. To further complicate things, secretion of acidic metabolites within biofilms can lead to degradation of disinfectants used in drinking water, which may facilitate microbe proliferation and detachment from the biofilm into the bulk water and enhance the potential for contaminated water (Emde et al. 1992, Starosvetsky et al. 2001). These concerns are further exacerbated by solubility differences of Pb(II) and Pb(IV) with different water chemistry, including pH and disinfectant residuals (Ahamed et al. 2020) that may lead to differential microbe-metal release potentials. This highlights the need for understanding the dynamics between biofilms and heavy metals in municipal plumbing systems to identify bacterial shifts with lead exposure and to determine if microbiological signatures might be a useful tool for diagnosing a previous lead exposure event even if there is no longer Pb exposure occurring.

To investigate the interactions between biofilms and heavy metal exposure and to examine if there is a dose-dependent effect of lead exposure on biofilm communities, we conducted a bench-scale experiment. Here, we investigated PEX-A (cross-linked polyethylene) and HDPE (high-density polyethylene) plastic pipes because of their flexibility, durability, corrosion resistance, and cost-effectiveness, which makes them popular for residential, commercial, and industrial plumbing systems. We investigated how Pb concentration impacted biofilm communities, biofilm biomass, and abundance of Pb-cycling genes within HDPE and PEX-A pipes. The main objective of this work was to ascertain if and how microbial communities shift in response to different concentrations of lead and across pipe types over time. In addition, we investigated whether we could detect previous lead exposure events, even if no lead is currently in the water, which may aid regulatory and public health officials in identifying previously undetected lead exposures. We anticipated that biofilm communities would be responsive to lead concentrations due to species-specific mortality, and responsive to pipe material given previous work suggests different biomass accumulation rates between PEX-A and HDPE (Ghoochani et al. 2023).

Materials and methods

Biofilm formation

Biofilms were established on virgin HDPE and PEX-A plastic pipes for 90 days using pipe loops connected to a municipal water supply in Memphis, TN, USA (Ghoochani et al. 2023, Hadiuzzaman et al. 2023). Individual pipe loops (Fig. S1) were established for each pipe material (HDPE and PEX-A) using three 2.7 m pipes per plastic type. These pipes were disinfected using chlorinated tap water (20 mg l^{-1} Cl_2) for 40 min followed by a 30-min flush with municipal tap water. These pipe loops were connected to municipal tap water supply (Memphis sands aquifer groundwater that was chlorinated for primary and secondary disinfection, aerated, filtered, and included orthophosphate (1 mg l^{-1}) as a corrosion inhibitor) for 90 days to allow natural biofilm establishment with a daily cycle of 16 h of flow and 8 h of stagnation at a flow rate of 2.0 l min^{-1} at room temperature. This growth regime was selected to emulate normal municipal premise water usage. After 90 days of biofilm development, individual pipe loops were constructed (Fig. 1) to test lead concentration effects.

Experimental design

Lead (Pb) standard solution (1000 mg l^{-1} in 3% nitric acid) for inductively coupled plasma mass spectrometry (ICP-MS) was used as a Pb source for this experiment (RICCA Chemicals, Arlington, TX, USA). After initial biofilm generation, individual pipe loops were constructed for each lead treatment level in triplicate. These pipes were exposed to different concentrations of lead with 0, 5, and 500 $\mu g\ l^{-1}$ in municipal tap water (pH adjusted to 7.8) for 4 and 8 weeks, followed by 4 weeks of Pb-free water (Fig. 1). Since biofilms within pipes might continually absorb lead (Hadiuzzaman et al. 2023), water was replaced every 5 days to ensure constant lead exposure. The terminal 4 weeks were conducted using Pb-free municipal water (pH adjusted to 7.8) for all pipes to emulate a post Pb-exposure environment as lead is slowly released from

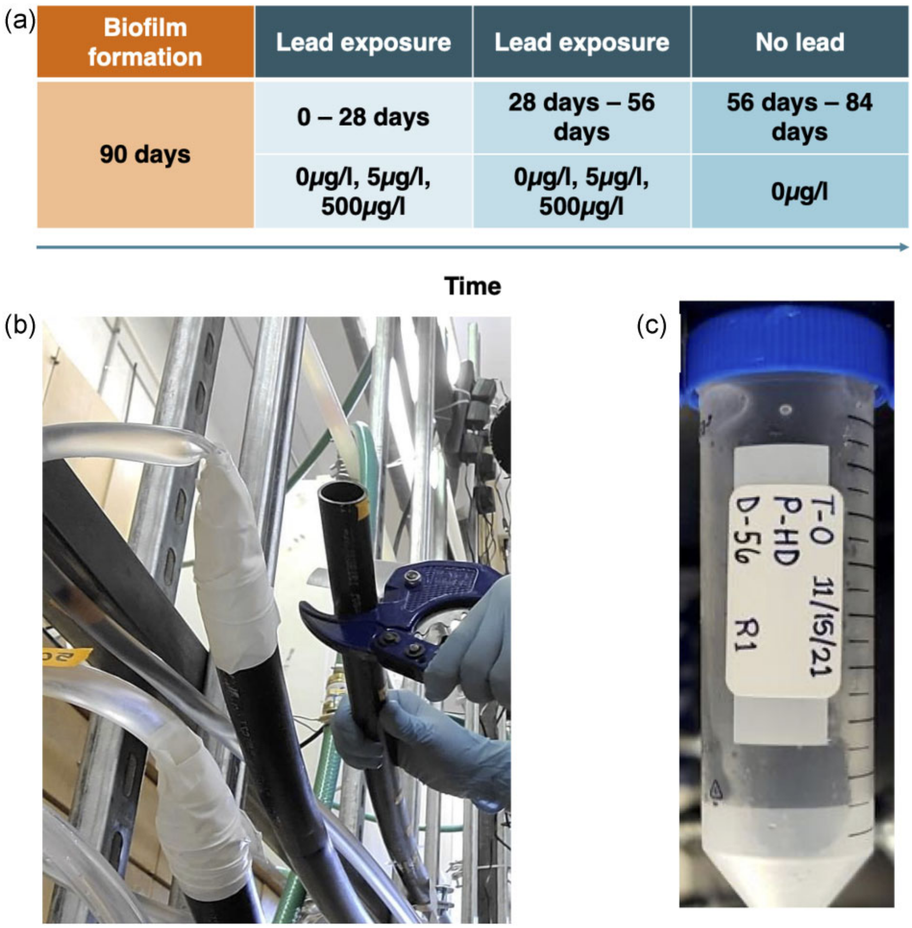

Biofilm formation	Lead exposure	Lead exposure	No lead
90 days	0 – 28 days	28 days – 56 days	56 days – 84 days
	0μg/l, 5μg/l, 500μg/l	0μg/l, 5μg/l, 500μg/l	0μg/l

Figure 1. Sampling scheme after initial 90-day biofilm at 28 and 56 days, followed by removal of lead for the terminal 4 weeks of the experiment with the final sample collected at 84 days (a). Also presented are images of pipe collection (b) and storage in 1× sterile PBS prior to extraction (c).

biofilms (Ghoochani et al. 2023), we deemed this a sufficient time for full lead release to examine community recovery.

Sample processing and DNA extraction

After each sampling time point (28, 56, and 84 days), individual pipe loops were temporarily disconnected, and 9 cm segments were cut and collected into sterile 50 ml centrifuge tubes and filled with sterile 1× PBS (Fig. 1) and pipe loops were reconnected for continued exposure by resealing tubing to the pipe loop. While this resulted in a change of flow and water pressure, the low flow rate used here is unlikely to dislodge biofilms as shear stresses would be minimal (Ghoochani et al. 2023). Biofilms were liberated from the interior surface of pipes via sonication (Branson 2800, Branson Ultrasonics, Brookfield CT, USA) at maximum oscillation for 10 min to aid separation followed by physical scraping (sterile single use stiff bristle brush for 5 min into 1× sterile PBS). The liberated biofilms were centrifuged at 5000 × g for 10 min at 4°C to pellet biofilms and the supernatant was removed (Seballos et al. 2020). Pelleted biofilms were resuspended in 500 μl of sterile molecular grade water and transferred into DNA extraction tubes. Total genomic DNA (gDNA) was extracted from biofilms using the PureLink® Genomic DNA Mini Kit (Invitrogen, Carlsbad, CA, USA) following standard procedures. Briefly, 200 μl of freshly prepared Lysozyme Digestion Buffer (20 mg ml^{-1}) was added to each sample, vortexed for 5 seconds, and incubated at 37°C for 30 min. The cells were harvested and resuspended in 180 μl PureLink® Genomic Digestion Buffer to lyse the cells with the addition of 20 μl Proteinase K and incubated at 55°C for 30 min to complete the lysis. Final gDNA was eluted in 100 μl of PureLink® Genomic Elution Buffer and quantified using Nanophotometer (N60; Implen, Munich, Germany). In total, we had 54 samples [two pipe types (HDPE and PEX-A), three concentrations (0, 5, and 500 μg l^{-1}), three time points (28, 56, and 84 days), and 3 replicates].

Metabarcoding

Metabarcoding libraries were generated using a two-step procedure (Brown et al. 2018) where primary PCR targeted the V4 region of the 16S rRNA gene operon using the primers 515F (Parada) and 806R (Apprill) (Parada, Needham and Fuhrman 2015; Apprill et al. 2015), which were synthesized to include the nexF and nexR Nextera sequencing primers and three ambiguous base pairs to enhance annealing efficacy for a final primer construct of nexF-NNN-515F and nexR-NNN-806R. Primary PCR consisted of 25 μl reactions and included Phusion Green Hot Start II High-Fidelity PCR Master Mix (12.5 μl; Thermo Fisher Scientific, Waltham, MS, USA), 2.5 μl of DNA template, 5.5 μl of molecular grade nuclease-free water, and 2.5 μl of each of the forward and reverse primers, with a total concentration of 1 μmol^{-1} of each primer; these

PCRs were conducted in duplicate. Primary PCR parameters were initially denaturated (98°C for 30 seconds), followed by 25 cycles of denaturation (98°C for 30 seconds), primer annealing (51°C for 20 seconds), and extension (72°C for 30 seconds), followed by a final extension at 72°C for 10 min. Ramp rate was 1.0°C s^{-1} for annealing stage and PCR results were visualized to confirm amplification using gel electrophoresis (1.5% agar w: v).

Secondary PCR consisted of the forward and reverse primer pairs P5-i5-nexF and P7-i7-nexR, which includes a distinct dual-barcode MIDs (i5 and i7), the Illumina Adaptor sequences (P5 and P7), and a partial overlap with the nexF and nexR sequences that act as annelation sites. Secondary PCRs were conducted in triplicate with unique barcodes. Secondary PCR reactions consisted of 12.5 μl Phusion Green Hot Start II High-Fidelity PCR Master Mix, 7.5 μl primary PCR product, 2.5 μl of molecular grade water, and 2.5 μl of dual-barcoded primer mix (0.5 μmol^{-1}) in 25 μl PCR reactions. Secondary PCR parameters were initial denaturation (98°C for 30 seconds), followed by 12 cycles of denaturation (98°C for 30 seconds), primer annealing (50°C for 20 seconds), and extension (72°C for 30 seconds), followed by a final extension at 72°C for 10 min. The final amplicon products were cleaned using 96 PCR Purification and Normalization Kit (Charm Biotech, Cape Girardeau, MO, USA) and pooled at equal concentrations per sample. Negative controls were included throughout and consisted of PCR reactions with molecular-grade water instead of DNA and these remained free from apparent contamination. The metabarcoding library was sequenced [Illumina MiSeq (300PE)] at the Integrated Genomics Facility, Manhattan, KS, USA. Sequences are accessioned in the NCBI SRA (BioProject PRJNA1268549; BioSamples SAMN48756718-SAMN48756796).

Quantitative biomass estimation and Pb-cycling gene quantification

Biomass estimation was conducted by quantifying 16S copies using Droplet Digital PCR (ddPCR) (following Hadiuzzaman et al. 2023). We acknowledge that this does not represent absolute quantification of biomass as several bacteria have multiple 16S regions per organism (Sun et al. 2013), but this method is often used to estimate microbial biomass as copy number variation is expected to be homogeneously distributed (Schill et al. 2024). Briefly, 20 μl reactions consisted of 125 nM of each primer 16S primer as above, 12.5 μl of QX200 ddPCR Evagreen Supermix (Bio-Rad, Hercules, CA, USA), 6.25 μl of gDNA (diluted in molecular grade water to 1:10–1:1000, optimized per sample), and molecular grade water up to 20 μl. Negative control consisting of molecular grade water were included in all reactions and were unamplified. Individual reactions were vortexed for 10 seconds and 20 μl of the mixed sample was transferred to the cartridge for droplet generation. The ddPCR parameters were enzyme activation at 95°C for 5 min, and 40 cycles of denaturation at 95°C for 30 seconds, dual annealing/extension at 60°C for 1 min, followed by signal stabilization at 4°C for 5 min, and 90 °C for 5 min. The ddPCR reactions were read using a QX200 Droplet Reader (Bio-Rad, Hercules, CA, USA) and analyzed for copy number per reaction QuantaSoft software (v.1.4, Bio-Rad, Hercules, CA, USA). The bacterial V4 copy numbers were normalized to the same area (mm^2 of pipe inner surface). Digital calipers (Fisher Brand Traceable, Waltham, MA, USA) were used to calculate the internal surface area of each pipe and total copy numbers/mm^2 were calculated.

To quantify genes within biofilms that have demonstrated involvement with Pb-cycling, we conducted ddPCR as above. MTs-encoding genes play a significant role in the process of metal detoxification and homeostasis (Robinson et al. 1990) and are useful to measure when investigating microbial-heavy metal processes in biofilms. The MT gene complex, *smt*, is comprised of two genes, *smtA* and *smtB*, which are translated in opposite directions (Huckle et al. 1993). The *bmtA* gene encodes a MT protein. We targeted the *smtAB* and *bmt* genes using the primers *smt1* and *smt2* (Naz et al. 2005) and *bmtF* and *bmtR* (Blindauer et al. 2002). We used ddPCR using the above parameters to quantify the copy numbers/mm^2 of these genes within each sample.

Sequence processing and statistical analyses

We used the program cutadapt (v.1.17; Martin 2011) to trim primer sequences from final amplicons and the program mothur (v.1.42.0; Schloss et al. 2009) was used for sequence processing (removing any ambiguous base pairs from contigs and any sequences with >12 homopolymers). Sequences were taxonomically classified using the Ribosomal Database Project (RDP) training set (v18) using a Naive Bayesian classifier (Wang et al. 2007) and reads not identified as bacteria, or belonging to mitochondrial or plastid groups, were removed. Retained sequences were demarcated into operational taxonomic units (OTUs) using the OptiClust algorithm (Westcott and Schloss 2017) at a 97% similarity threshold. OTUs with fewer than 10 reads globally were potentially spurious and were removed before analyses (Brown and Jumpponen 2015, Oliver et al. 2015), and consensus taxonomic classifications and representative sequences were produced for each OTU.

Richness (relative observed richness—S_{obs}), diversity (Simpson's 1-D), evenness (Simpson's—E_D), and Bray–Curtis dissimilarity values were estimated via iterative subsampling whereby we subsampled each experimental unit to a sequence depth of 15 000 sequences using 1000 iterations, and the average values were used for all downstream analyses. For diversity estimates (S_{obs}, 1-D, and E_D), we tested if our experimental framework impacts these estimates using ANOVA with the model sampling time, lead concentration, and pipe type with all possible interactions.

To test if biofilm communities were structurally different across our experimental framework, we used the model-based multivariate framework using the R package *mvabund* (v.4.2.1; Wang et al. 2012), which fits separate generalized linear models for abundance data for each OTU against a distribution (negative binomial used here) and integrates these across all OTUs to test if the community deviates from expected distributions using Analyses of Deviance tests for the model lead concentration, pipe material, time of exposure, and all possible three-way interactions with 999 bootstrap iterations using PIT-trap resampling and Likelihood-Ratio-Tests. To visualize community differences, we conducted nonmetric multidimensional scaling (NMDS) as conducted by mothur using 1000 iterations and the best solution was selected (highest R^2).

We constructed a series of stacked histograms of relative abundances to visualize diversity at the phylum and order levels by condition (e.g. pipe type, lead concentrations, and time interval). Additionally, we wanted to identify OTUs that may serve as biomarker taxa for lead exposure events. To do so, we used the program LEfSe (Segata et al. 2011) using lead concentration (0, 5, and 500 μg l^{-1}) as the class and pipe material (HDPE and PEX-A) as subclass to identify lead responsive biomarker taxa whist accounting for variation associated with pipe material. For all identified biomarker taxa (see results), we further investigated temporal dynamics of each of these OTUs to understand how these biomarker taxa were impacted by lead exposure and time. To do this, we conducted a series of analyses using relative abundances of each OTU as a response variable; a one-way ANOVAs (treating sampling dates as categories) and segmented regression [R package *segmented* (Muggeo 2008)] using the 8 week sampling point as a break point. Additionally, recent work has identified key globally distributed taxa in water distribution systems, specifically Candidatus *Raskinella chloraquaticus* which has been previously misidentified as a member of the order Rhizobiales due do similar 16S identities (Sudarshan et al. 2024). Since we had several taxa belong to Rhizobiales included in observed biomarker taxa (see below), we wanted to test of our Rhizobiales belonged to this key global taxon. We downloaded the assembled Candidatus *Raskinella chloraquaticus* genome (UBA383; GCF_002298295.1) from NCBI, extracted the 16S ribosomal region using the program barrnap (v.0.9) and compared these to our 16S sequences for Rhizobiales using BLASTn (NCBI) and none of our obtained OTUs were this globally abundant taxa (max % identity = 90.12%).

To test if microbial biomass (16S copy numbers) within biofilms and the occurrence of lead modulation genes (*smtAB* and *bmt*) we conducted a three-way ANOVA with subsequent Tukey HSD post hoc tests and a series of logistic regressions (presence/absence of gene as detected using ddPCR) for each pipe material separately, respectively using Pb concentration as the independent variable.

All statistics and analyses were conducted using a combination of JMP Pro (v14.1; SAS Institute, Cary, NC), R (v.4.2.3), and mothur (v.1.42.0).

Results

Biofilm community responses

After sequence quality control, we were left with 10 293 728 sequences that were demarcated into 1144 OTUs. Full taxonomic and abundance results for each OTUs is presented in Table S1. We see that our experimental framework differentially impacted diversity estimates within our biofilms. While biofilm richness was not impacted by our experimental design ($F_{17,53} = 1.135$, $P = 0.361$), we see that both diversity (1-D) and evenness are ($F_{17,53} = 3.705$, $P < 0.001$, $F_{17,53} = 3.213$, $P = 0.002$, respectively). Further, we see that pipe material, pipe by time interactions, and pipe by time by concentration interactions are significant in our effects tests. Tukey HSD posthoc tests indicate that this is driven by increased diversity and evenness in HDPE compared to PEX-A.

Using model-based tests of community structure (*mvabund*), we see that all experimental factors and interactions influenced the structure of these biofilm communities (Table 1). While all factors influenced community structure, visualization of community structure via NMDS (Fig. 2) suggests that communities appear to shift most strongly across time for both pipe types, particularly with NMDS Axis 1 which explained >70% of the community variation. We also see an expansion of community variation at the day 56 sample followed by a reduction in community variation at day 84 as evidenced in datapoint spread in ordination space.

Table 1. Results of multivariate analyses of deviance based on negative binomial distribution for combine error calculations.

Treatment Factors	Residual df	Factor df	Deviance	*P*-value
Intercept	53			
Pb concentration	51	2	10055	0.001
Time	49	2	4914	0.002
Pipe material	48	1	8850	0.001
Pb × time	44	4	7317	0.001
Pb × pipe	42	2	4578	0.001
Time × pipe	40	2	4057	0.001
Pb × time × pipe	36	4	8079	0.004

Presented are treatments, residual and treatment factor degrees of freedom, deviance test statistic, and associated *P*-value.

Visualization of taxonomic composition at the phyla level (Fig. 3a,b) indicated that Proteobacteria (we use the synonym Proteobacteria over the more recent pseudomonadota as this taxonomic identity used in the taxonomic training set) was found to be the most abundant phylum across different samples and there was a gradual increase of Bacteroidetes from 56 days in different concentrations in PEX pipes. Similarly, in HDPE pipes (Fig. 3b) Proteobacteria dominated in most of the conditions but conversely, Bacteroidetes was present in the initial days of the experiment in different conditions of lead. Similarly, bacterial orders were visualized (Fig. 4a,b) and Sphingomonadales was found to be the most abundant order across both pipe types.

Individual biomarker taxa

Analyses of biomarker taxa for lead exposure identified seven OTUs that were biomarkers of a particular lead concentration (see Table S2 for full statistics). These include biomarker taxa for high lead concentration (500 μg l^{-1}; OTU30 (LDA = 3.354, $P < 0.001$; *Sphingopyxis* sp., Proteobacteria, Sphingomonadaceae), OTU43 (LDA = 3.085, $P < 0.001$; *Rhizobium* sp., Proteobacteria, Rhizobiaceae), OTU59 [LDA = 2.979, $P = 0.033$; bacteria (unclassified), OTU69 (LDA = 2.734, $P < 0.001$; *Noviherbaspirillum* sp., Proteobacteria, Oxalobacteraceae), and OTU86 (LDA = 2.688, $P < 0.001$; *Sphingomonas* sp., Proteobacteria, Sphingomonadaceae)], moderate lead concentration (5 μg l^{-1}; OTU114, LDA = 2.130, $P = 0.003$), and no lead (0 μg l^{-1}; OTU23, LDA = 3.674, $P < 0.001$). As lead was removed from the system after 8 weeks, we investigated how this removal impacted the relative abundances of these biomarker taxa. All these biomarker taxa had consistent relative abundances even after lead was removed from the system based on results from ANOVAs (Table 2), but one OTU (OTU23) did decrease in relative abundance across time based on regression analyses when data is treated quantitatively (Table 2). Furthermore, while we tested OTUs using segmented regression at the 56-days break point, no OTUs had a significant break point.

Quantification of biofilm biomass and Pb-associated genes

The results showed that the biomass of biofilms formed on PEX-A pipes were lower ($3.08 \times 10^6 \pm 1.57 \times 10^6$ copies cm^{-2}, mean ± SD) than HDPE pipes

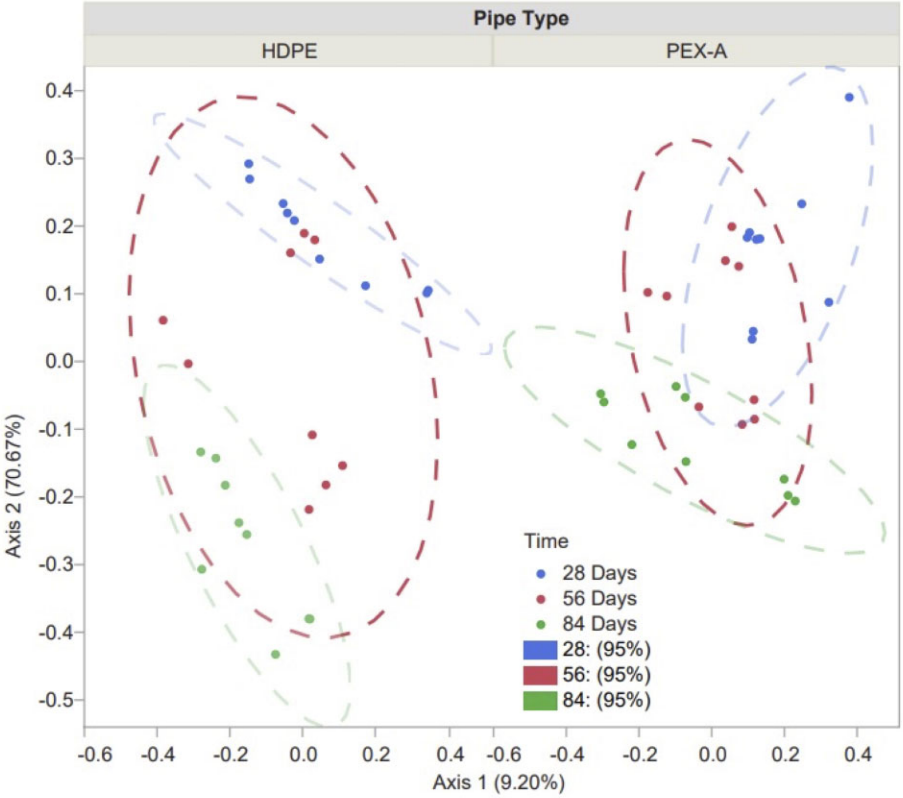

Figure 2. Nonmetric multidimensional scaling plot visualizing community structure of biofilms across the two most explanatory axes. Presented are communities separated by pipe material (HDPE on left and PEX-A on right) and color coded by sampling date with 95% confidence ellipses (dashed).

($1.09 \times 10^7 \pm 2.81 \times 10^7$ copies cm^{-2}, mean ± SD). The inner surface of HDPE pipes often has a rougher surface than PEX-A pipes, facilitating microbes to attach to form of thicker biofilms. Results indicate that biomass does not change with time, lead concentration, or their interaction for either PEX-A pipes ($F_{8,26} = 1.197$, $P = 0.353$) or HDPE pipes ($F_{8,26} = 0.974$, $P = 0.485$).

Investigations into the occurrence of Pb-cycling genes demonstrated that these genes were conditionally rare and either there were no detected *smtAB* or *bmt* genes or these were detected with very low copy numbers, but only under certain conditions. These MT genes have been most commonly studied in soils (Naik et al. 2012, Chatterjee et al. 2020, Wang et al. 2022), and their low detection may be because municipal water-originated biofilms consist of few taxa that have these genes, but these may be strongly upregulated in presence of Pb (Chaturvedi et al. 2012, Kimari and Das 2019). However, given that they were found in different abundances in different pipes and/or lead exposure events, it is most likely that chemical interactions drive abundance of these genes in our system. The *smtAB* gene was only detected in low or no lead conditions (i.e. 0 and 5 µg l^{-1}) in HDPE pipes but was abundant in PEX-A across all three concentrations (Fig. S4a,b). While the proportion of samples in which we detected the *smtAB* gene did not differ with Pb concentration in PEX-A pipes (Fig. S4b), in HDPE pipes, the probability of detecting *smtAB* genes increased with increasing lead concentration (Fig. S4a; $\chi^2 = 4.407$, $P = 0.036$). Analyses of the *bmt* gene indicated similar but contrasting patterns as the *smtAB* gene. We see that *bmt* was more likely to be detected in lower or no lead concentrations in HDPE pipes (Fig. S5a; $\chi^2 = 0.772$, $P = 0.038$) while the probability of detection in the *bmt* gene did not change in PEX-A pipes (Fig. S5b).

Discussion

Biofilms on pipe surfaces may result in deterioration of drinking water quality and might act as a source of lead release long after a lead exposure event. Given that there is little known about biofilm-heavy metal interactions within plastic potable water pipes, we conducted an innovative bench-scale experiment to investigate this. We tested if lead exposure dose-dependently affected HDPE and PEX-A pipe bacterial communities over time. Using multiple lines of evidence, we found that bacterial biofilm communities were impacted by lead concentration, pipe material, and time, and we identified several key taxa that are apparently diagnostic of high lead environments and can be considered biomarkers. Importantly, these taxa persisted in their relative abundance even 4-weeks after lead removal. This provides the strongest evidence to date that Pb-induced changes in bacterial communities persist long after a lead exposure event. This is a necessary first step toward developing alternative lead exposure monitoring regimes and suggests that it is possible to use biomarker taxa as a triage and/or diagnostic tool of a previous lead exposure event in water, even after lead is no longer in the system. While there is much additional work needed to develop microbe/microbiome-enabled monitoring tools, this work provides a path forward toward triage capability whereby using microbial responses, we may be able to provide water managers and health officials evidence that there may have been a previously undetected lead-water

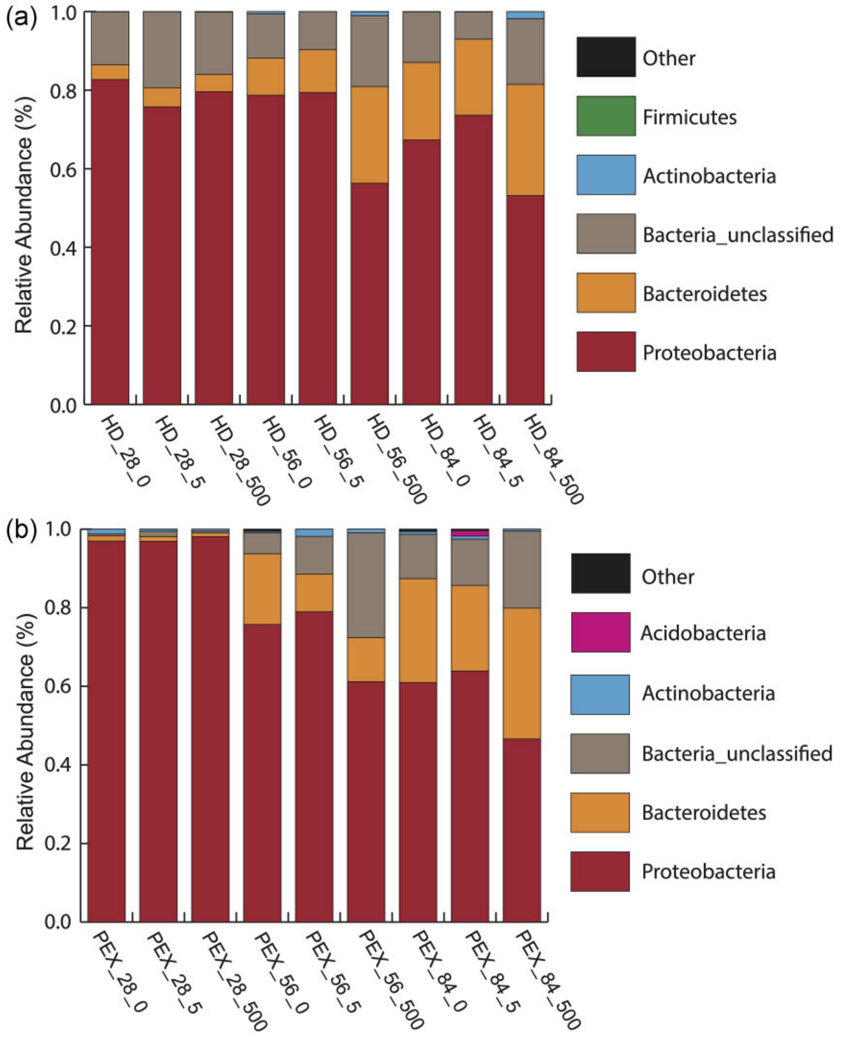

Figure 3. Stacked histogram of identified phyla in HDPE (a) and PEX-A (b) pipes across samples for different lead treatments and time intervals based on the relative abundances of the communities. HD—HDPE pipes, PEX—PEX-A pipes; 28, 56, and 84 in the sample label represents days since initial Pb exposure; 0, 5, and 500 in the sample label represents Pb-exposure concentrating.

exposure event so they can initiate monitoring or testing procedures they deem appropriate.

Biofilms formed by the microbes present in the drinking water distribution system can shelter pathogens, degrade organic matter, and alter aesthetic properties of tap water (Sudarshan et al. 2024). Despite the advancements in water quality regulation, the interaction between biofilms and heavy metals, such as lead, in premise plumbing systems poses significant public health risks, including the potential for persistent heavy metal contamination, is inadequately comprehended. Further, the phyla Proteobacteria and Bacteroidetes, which were the most abundant phyla found (Fig. 3), are large drivers of antibiotic resistance horizontal gene transfer. While testing for presence of antibiotic resistance genes was beyond the scope of this current work, this may be a worthwhile avenue of study in the future as these bacteria are very likely to be ingested.

We identified strong community shifts and biomass differences between PEX-A and HDPE pipes with HDPE pipes having an order of magnitude higher biomass (proxied by 16S copy numbers) than PEX-A. These biomass differences are interesting as biomass estimations using similar pipe loop frameworks have contrasting results; some suggest PEX-A houses higher biomass (Ghoochani et al. 2023, Hadiuzzaman et al. 2023), whereas some are congruent with our current study with HDPE having higher biomass (Datta et al. 2025). HDPE often has more hydrophobicity in comparison to PEX-A and the microorganisms that exhibit a hydrophobic preference have a higher affinity for adhering to HDPE surfaces, leading to a boosted accumulation of biomass. PEX-A's hydrophilic nature can potentially reduce microbe adhesion and biofilm formation (Ghabeche et al. 2019). This suggests that biofilm development dynamics are likely mainly stochastic and driven largely by founder effects ultimately structured by local source water and environmental conditions. Furthermore, while the causes of the differences in biofilm communities between these two common water pipe materials grown simultaneously in the same pipe loop are unknown, previous work suggests likely mechanisms. It has been demonstrated using optical profilometry (Datta et al. 2025), that surface roughness of new HDPE pipes is markedly higher than that of PEX-A pipes which should facilitate initial adhesion of different bacteria during biofilm development. This, coupled with differential surface loading and binding energy values as related with Pb^{+} ions between the two plastic types (Datta et al. 2025) and

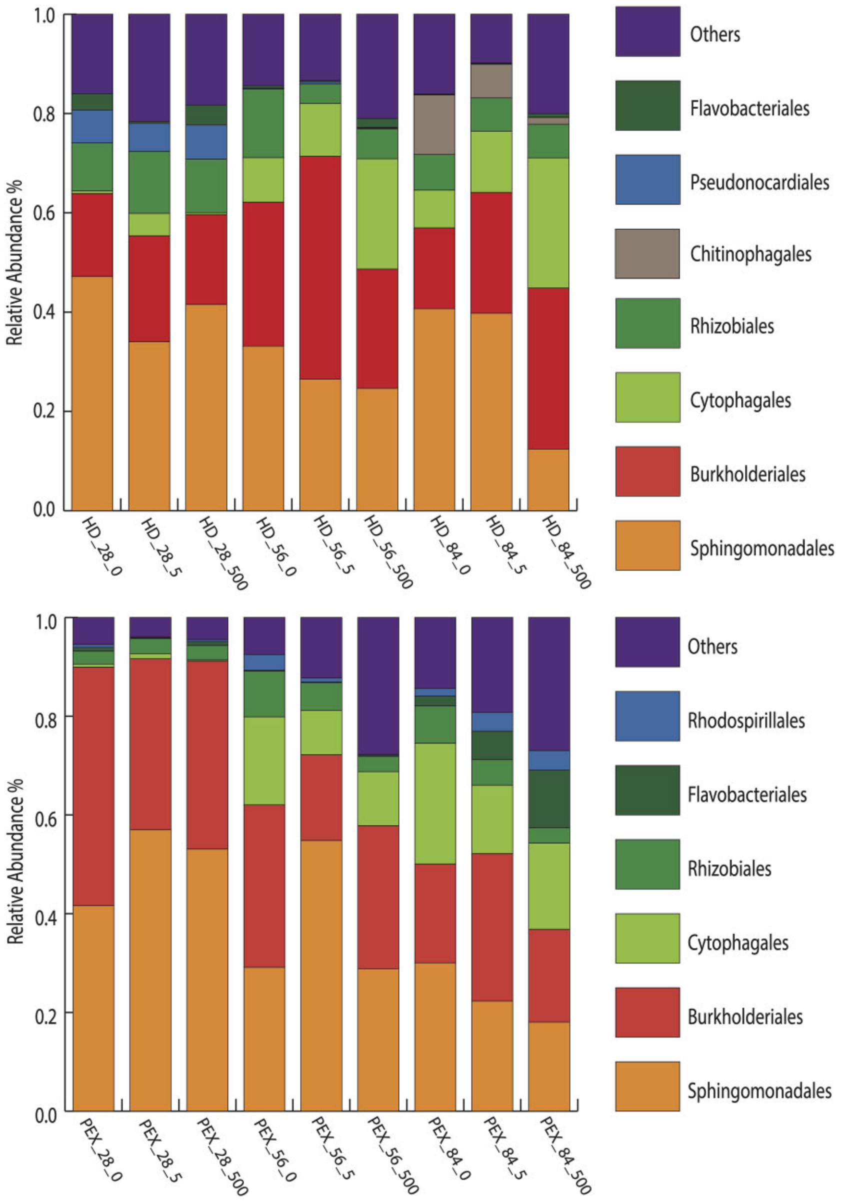

Figure 4. Stacked histogram of identified orders in HDPE (top) and PEX-A (bottom) pipes across samples for different lead treatments and time intervals based on the relative abundances of the communities. HD—HDPE pipes, PEX—PEX-A pipes; 28, 56, and 84 in the sample label represents days since initial Pb exposure; 0, 5, and 500 in the sample label represents Pb-exposure concentrating.

Table 2. Identified Biomarker taxa (LEfSe) associated with various lead concentrations including OTU name and lowest taxonomic rank determined.

OTU ID	Taxonomic ID	ANOVA results	Regression
OTU23	*Methylobacterium*	$F_{2,17} = 3.385$, $P = 0.061$	t=-2.400, $P = 0.028$
OTU30	*Sphingopyxis*	$F_{2,17} = 0.3629$, $P = 0.7016$	t= -0.855, $P = 0.4053$
OTU43	Rhizobiaceae (unclassified)	$F_{2,17} = 0.7179$, $P = 0.5038$	t= -1.191, $P = 0.251$
OTU59	Bacteria (unclassified)	$F_{2,17} = 1.0133$, $P = 0.3866$	t= -1.259, $P = 0.2262$
OTU69	*Noviherbaspirillum*	$F_{2,17} = 1.0414$, $P = 0.3771$	t= -1.27, $P = 0.2222$
OTU86	*Sphingomonas*	$F_{2,17} = 1.1538$, $P = 0.3419$	t = 0.743, $P = 0.4684$
OTU114	Caulobacteraceae (unclassified)	$F_{2,17} = 1.0443$, $P = 0.3762$	t= -1.199, $P = 0.2481$

Also presented are AVOVA (F statistic and P values) and regression analyses (t statistic and *P*-values) results tests changes in relative abundance over time.

different contaminate saturation half-life and solubility between HDPE and PEX-A (Whelton et al. 2010) driven by differences in their molecular structures, might help explain why communities differed between the pipe types in our experiment. The persistence of communities after removal of lead exposure pressures may be due to unique viscoelastic dynamics of these biofilms (Gloag et al. 2020), which may result in coalescence of lead resistant biofilms after exposure, thus leading to stable recovered communities.

We identified several biomarker taxa that were overrepresented in pipes with lead exposure, most of which (five) were biomarkers of extreme lead concentrations (500 μg l^{-1} Pb) and one from lower lead concentrations (5 μg l^{-1} Pb) and all of these had consistent abundances after lead removal. These OTUs include members of the genera *Sphingopysix, Noviherbaspirillum, Sphingomonas*, and a Rhizobiaceae sp., which might be target taxa that are indicative of a previous lead exposure event and are worth exploring further. One of these taxa, *Sphingopyxis* is a member of the family Sphingomonadaceae, and are often found in low-nutrient, oligotrophic environments that are often found in stagnant conditions in tap water, chlorinated and nonchlorinated drinking water systems, and premise plumbing biofilms (Ling et al. 2018). *Sphingopyxis* and *Sphingomonas* both produce sphingolipids and glycosphingolipids in their cell envelopes, contributing to membrane stability and environmental resilience (Gomez-Alvarez et al. 2016), and may play a significant role in pollutant degradation and metabolic flexibility (Aylward et al. 2013). *Noviherbaspirillum* is in the family Oxalobacteraceae and is underexplored and likely has the ability to resist metals, form biofilms, engage in denitrification, and adapt in low-oxygen environments (Rajkumar et al. 2009).

One of the major findings of this work is that biofilm communities not only respond to lead exposure but also retain lead-responsive biomarker taxa even after lead removal. Adaptations of these biomarker taxa to prolonged lead exposure without mortality and DNA degradation is interesting and requires further exploration. Based upon the previous literature, many common taxa present in drinking water distribution systems have resilient qualities, including the capability to form biofilms, diverse metabolic capabilities, chlorine resistance, and varied nutrient cycling capabilities (Sudarshan et al. 2024). Given that we detected lead-modulating genes in our ddPCR analyses, and these were responsive to lead concentrations, this implies biological functionality rather than residual DNA presence. This suggests that certain microbial communities have developed resilience strategies that enable them to thrive in environments contaminated with lead. Additional work is needed understand the mechanisms of these Pb-resistant gene responses in municipal potable waters, including investigating additional gene families beyond MT, such as metal efflux pumps genes (Sanchez-Corona et al. 2025), and how Pb exposure regulates gene expression at different Pb concentrations. Studying these adaptive mechanisms in the future could help us better understand ways to use microbes for bioremediation efforts.

The identification of lead-responsive biomarker taxa offers valuable insights for developing diagnostic tools to assess past lead exposure incidents. These tools could support health officials in identifying contamination sources and provide proactive lead monitoring options. One thing that could support this is the development of a comprehensive database of lead-responsive microbial taxa across various plumbing materials and water systems, and establishing standardized techniques for biomarker detection, encompassing DNA-based tests and functional gene analyses. Such tools could help water distribution management groups and community, state, and federal health organizations identify prior lead exposure occurrences, improving community health outcomes. This study provides proof of concept that microbiome monitoring is a promising tool that may detect a nonrecurring lead exposure episode. Additionally, this research into lead-modulating genes (e.g. *smtAB* and *bmt*) emphasizes the importance for biofilms to modulate lead toxicity through sequestration and detoxification mechanisms. The gene prevalences varied by pipe material and lead concentration, suggesting specific microbial adaptations to environmental conditions. More research is needed to refine these tools, but this promising area suggests a novel way to identify potential lead exposure events even after an active lead event.

Acknowledgments

The authors would also like to thank Amy Abell and Nathan Mullins in the Department of Biological Sciences at the University of Memphis for their assistance in conducting ddPCR-based biomass quantification and Avery Tucker for assistance in sampling. This work did not have human or animal subjects.

Author contributions

Nahreen Mirza (Conceptualization, Data curation, Formal analysis, Investigation, Methodology, Visualization, Writing – original draft, Writing – review & editing), Md Hadiuzaman (Methodology, Writing – review & editing), David A. Ladner (Conceptualization, Funding acquisition, Writing – review & editing), Maryam Salehi (Conceptualization, Funding acquisition, Methodology, Writing – review & editing), and Shawn P. Brown (Conceptualization, Data curation, Formal analysis, Funding acquisition, Investigation, Methodology, Supervision, Writing – original draft, Writing – review & editing)

Supplementary data

Supplementary data is available at *JAMBIO Journal* online.

Conflict of interest: None declared.

Funding

Funding for this work was provided by the National Science Foundation (NSF) grant CBET-2029764 to M.S. and S.P.B.

Data availability

The data supporting the findings of this study are available from the corresponding author upon reasonable request. Sequences are accessioned in the NCBI SRA (BioProject PRJNA1268549; BioSamples SAMN48756718-SAMN48756796).

References

Ahamed T, Brown SP, Salehi M. Investigate the role of biofilm and water chemistry on lead deposition onto and release from polyethylene: an implication for potable water pipes. *J Hazard Mater* 2020;400:123253. https://doi.org/10.1016/j.jhazmat.2020.123253

Apprill A, McNally S, Parsons R, Weber L. Minor revision to V4 region SSU rRNA 806R gene primer greatly increases detection of SAR11 bacterioplankton. *Aquatic Microbial Ecology* 2015;75:129–137. https://doi.org/10.3354/ame01753

Aylward FO, McDonald BR, Adams SM *et al.* Comparison of 26 Sphingomonad genomes reveals diverse environmental adaptations and biodegradative capabilities. *Appl Environ Microb* 2013;**79**:3724–33. https://doi.org/10.1128/AEM.00518-13

Blindauer CA, Harrison MD, Robinson AK *et al.* Multiple bacteria encode metallothioneins and SmtA-like zinc fingers. *Mol Microbiol* 2002;**45**:1421–32. https://doi.org/10.1046/j.1365-2958.2002.03109.x

Brown SP, Leopold DR, Busby PE. Methods in Molecular Biology. In: Ma W, Wolpert T. (eds.), *Plant Pathogenic Fungi and Oomycetes*. Springer, 2018, 39–51. https://doi.org/10.1007/978-1-4939-8724-5_4

Brown SP, Jumpponen A. Phylogenetic diversity analyses reveal disparity between fungal and bacterial communities during microbial primary succession. *Soil Biol Biochem* 2015;**89**:52–60. https://doi.org/10.1016/j.soilbio.2015.06.025

Buse HY, Lu J, Lu X *et al.* Microbial diversities (16S and 18S rRNA gene pyrosequencing) and environmental pathogens within drinking water biofilms grown on the common premise plumbing materials unplasticized polyvinylchloride and copper. *FEMS Microbiol Ecol* 2014;**88**:280–95. https://doi.org/10.1111/1574-6941.12294

Calero Preciado C, Soria-Carrasco V, Boxall J *et al.* Climate change and management of biofilms within drinking water distribution systems. *Front Environ Sci* 2022;**10**:962514. https://doi.org/10.3389/fenvs.2022.962514

Calomiris JJ, Armstrong JL, Seidler RJ. Association of metal tolerance with multiple antibiotic resistance of bacteria isolated from drinking water. *Appl Environ Microb* 1984;**47**:1238–42. https://doi.org/10.1128/aem.47.6.1238-1242.1984

Chatterjee S, Kumari S, Rath S *et al.* Diversity, structure and regulation of microbial metallothionein: metal resistance and possible applications in sequestration of toxic metals. *Metallomics* 2020;**12**:1637–55. https://doi.org/10.1039/d0mt00140f

Chaturvedi AK, Mishra A, Tiwari V *et al.* Cloning and transcript analysis of type 2 metallothionein gene (SbMT-2) from extreme halophyte *Salicornia brachiata* and its heterologous expression in *Escherichia coli*. *Gene* 2012;**499**:280–7. https://doi.org/10.1016/j.gene.2012.03.001

Council NR. *Drinking water distribution systems: assessing and reducing risks. Executive summary*. Washington DC: National Research Council, 2010.

Datta DK, Paramban S, Yazdani H *et al.* Influence of biofilm and calcium carbonate scaling on lead transport in plastic potable water pipes: a laboratory and molecular dynamics study. *J Hazard Mater* 2025;**485**:136831. https://doi.org/10.1016/j.jhazmat.2024.136831

Egea LG, Brun FG, Jiménez-Ramos R. Dissolved organic carbon leaching from microplastics and bioavailability in coastal ecosystems. *Sci Total Environ* 2024;**909**:168673. https://doi.org/10.1016/j.scitotenv.2023.168673

Emde K, Smith DW, Facey R. Initial investigation of microbially influenced corrosion (MIC) in a low temperature water distribution system. *Water Res* 1992;**26**:169–75. https://doi.org/10.1016/0043-1354(92)90216-Q

Feazel LM, Baumgartner LK, Peterson KL *et al.* Opportunistic pathogens enriched in showerhead biofilms. *Proc Natl Acad Sci USA* 2009;**106**:16393–9. https://doi.org/10.1073/pnas.0908446106

Flemming HC, Percival SL, Walker JT. Contamination potential of biofilms in water distribution systems. *Water Supply* 2002;**2**:271–80. https://doi.org/10.2166/ws.2002.0032

Ghabeche W, Chaoui K, Zeghib N. Mechanical properties and surface roughness assessment of outer and inner HDPE pipe layers after exposure to toluene methanol mixture. *Int J Adv Manuf Technol* 2019;**103**:2207–25. https://doi.org/10.1007/s00170-019-03651-z

Ghoochani S, Hadiuzzaman M, Mirza N *et al.* Effects of water chemistry and flow on lead release from plastic pipes versus copper pipes: implications for plumbing decontamination. *Environ Pollut* 2023;**337**:122520. https://doi.org/10.1016/j.envpol.2023.122520

Gloag ES, Fabbri S, Wozniak DJ *et al.* Biofilm mechanics: implications in infection and survival. *Biofilm* 2020;**2**:100017. https://doi.org/10.1016/j.bioflm.2019.100017

Gomez-Alvarez V, Pfaller S, Revetta RP. Draft genome sequence of two *Sphingopyxis* sp. strains, dominant members of the bacterial community associated with a drinking water distribution system simulator. *Genome Announc* 2016;**4**:e00183–16.

Hadiuzzaman M, Mirza N, Brown SP *et al.* Lead (Pb) deposition onto new and biofilm-laden potable water pipes. *Chemosphere* 2023;**342**:140135. https://doi.org/10.1016/j.chemosphere.2023.140135

Huckle JW, Morby AP, Turner JS *et al.* Isolation of a prokaryotic metallothionein locus and analysis of transcriptional control by trace metal ions. *Mol Microbiol* 1993;**7**:177–87. https://doi.org/10.1111/j.1365-2958.1993.tb01109.x

Ibekwe AM, Murinda SE. Linking microbial community composition in treated wastewater with water quality in distribution systems and subsequent health effects. *Microorganisms* 2019;**7**:660. https://doi.org/10.3390/microorganisms7120660

Kim EJ, Herrera JE. Characteristics of lead corrosion scales formed during drinking water distribution and their potential influence on the release of lead and other contaminants. *Environ Sci Technol* 2010;**44**:6054–61. https://doi.org/10.1021/es101328u

Kumari S, Das S. Expression of metallothionein encoding gene bmtA in biofilm-forming marine bacterium *Pseudomonas aeruginosa* N6P6 and understanding its involvement in Pb(II) resistance and bioremediation. *Environ Sci Pollut Res* 2019;**26**:28763–74. https://doi.org/10.1007/s11356-019-05916-2

Lautenschlager K, Boon N, Wang Y *et al.* Overnight stagnation of drinking water in household taps induces microbial growth and changes in community composition. *Water Res* 2010;**44**:4868–77. https://doi.org/10.1016/j.watres.2010.07.032

Lee D, Calendo G, Kopec K *et al.* The impact of pipe material on the diversity of microbial communities in drinking water distribution systems. *Front Microbiol* 2021;**12**:779016. https://doi.org/10.3389/fmicb.2021.779016

Ling F, Whitaker R, LeChevallier MW *et al.* Drinking water microbiome assembly induced by water stagnation. *ISME J* 2018;**12**:1520–31. https://doi.org/10.1038/s41396-018-0101-5

Martin Marcel. Cutadapt removes adapter sequences from high-throughput sequencing reads. *EMBnet.journal* 2011;**17**:10. https://doi.org/10.14806/ej.17.1.200

Montagnino E, Proctor CR, Ra K *et al.* Over the weekend: water stagnation and contaminant exceedances in a green office building. *PLOS Water* 2022;**1**:e0000006. https://doi.org/10.1371/journal.pwat.0000006

Muggeo VMR. Segmented: an R package to fit regression models with broken-line relationships. *R News* 2008;**8**:20–5.

Naik MM, Shamim K, Dubey SK. Biological characterization of lead-resistant bacterial to explore role of bacterial metallothionein in lead resistance. *Current Sci* 2012;**4**:426–9.

Naz N, Young HK, Ahmed N *et al.* Cadmium accumulation and DNA homology with metal resistance genes in sulfate-reducing bacteria. *Appl Environ Microb* 2005;**71**:4610–18. https://doi.org/10.1128/AEM.71.8.4610-4618.2005

Neu L, Hammes F. Feeding the building plumbing microbiome: the importance of synthetic polymeric materials for biofilm formation and management. *Water* 2020;**12**:1774. https://doi.org/10.3390/w12061774

Nong Q, Yuan K, Li Z *et al.* Bacterial resistance to lead: chemical basis and environmental relevance. *J Environ Sci* 2019;**85**:46–55. https://doi.org/10.1016/j.jes.2019.04.022

Oliver AK, Brown SP, Callaham MA *et al.* Polymerase matters: non-proofreading enzymes inflate fungi community richness estimates by up to 15%. *Fungal Ecol* 2015;**15**:86–89. https://doi.org/10.1016/j.funeco.2015.03.003

Parada AE, Needham DM, Fuhrman JA. Every base matters: assessing small subunit rRNA primers for marine microbiomes with mock communities, time series and global field samples. *Environmental*

Microbiology 2015;**18**:1403–14. https://doi.org/10.1111/1462-2920.13023

Proctor CR, Dai D, Edwards MA *et al*. Interactive effects of temperature, organic carbon, and pipe material on microbiota composition and *Legionella pneumophila* in hot water plumbing systems. *Microbiome* 2017;**5**:130. https://doi.org/10.1186/s40168-017-0348-5

Raghupathi PK, Liu W, Sabbe K *et al*. Synergistic interactions within a multispecies biofilm enhance individual species protection against grazing by a pelagic protozoan. *Front Microbiol* 2017;**8**:2649. https://doi.org/10.3389/fmicb.2017.02649

Rajkumar M, Ae N, Freitas H. Endophytic bacteria and their potential to enhance heavy metal phytoextraction. *Chemosphere* 2009;**77**:153–60. https://doi.org/10.1016/j.chemosphere.2009.06.047

Robinson NJ, Gupta A, Fordham-Skelton AP *et al*. Prokaryotic metallothionein gene characterisation and expression: chromosome crawling by ligation-mediated PCR. *Proc Biol Sci* 1990;**242**:241–7.

Romera-Castillo C, Pinto M, Langer TM *et al*. Dissolved organic carbon leaching from plastics stimulates microbial activity in the ocean. *Nat Commun* 2018;**9**:1430. https://doi.org/10.1038/s41467-018-03798-5

Rosen MB, Pokhrel LR, Weir MH. A discussion about public health, lead and *Legionella pneumophila* in drinking water supplies in the United States. *Sci Total Environ* 2017;**590-591**:843–52. https://doi.org/10.1016/j.scitotenv.2017.02.164

Salehi M, DeSimone D, Aghilinasrollahabadi K *et al*. A case study on tap water quality in large buildings recommissioned after extended closure due to the COVID-19 pandemic. *Environ Sci: Water Res Technol* 2021;**7**:1996–2009. https://doi.org/10.1039/D1EW00428J

Sánchez-Corona CG, Gonzalez-Avila LU, Hernández-Cortez C *et al*. Impact of heavy metal and resistance genes on antimicrobial resistance: ecological and public health implications. *Genes* 2025;**16**:625. https://doi.org/10.3390/genes16060625

Schill ML, Baird R, Brown SP *et al*. Wildfire severity alters soil microbial exoenzyme production and fungal abundances in the Southern Appalachian Mountains. *Pedosphere* 2024;**34**:865–78. https://doi.org/10.1016/j.pedsph.2023.05.008

Schloss PD, Westcott SL, Ryabin T *et al*. Introducing mothur: Open-Source, Platform-Independent, Community-Supported Software for Describing and Comparing Microbial Communities. *Applied and Environmental Microbiology* 2009;**75**:7537–41. https://doi.org/10.1128/AEM.01541-09

Seballos RC, Wyatt KH, Bernot RJ *et al*. Nutrient availability and organic matter quality shape bacterial community structure in a lake biofilm. *Aquat Microb Ecol* 2020;**85**:1–18. https://doi.org/10.3354/ame01937

Segata N, Izard J, Waldron L *et al*. Metagenomic biomarker discovery and explanation. *Genome Biol* 2011;**12**:R60. https://doi.org/10.1186/gb-2011-12-6-r60

Starosvetsky D, Armon R, Yahalom J *et al*. Pitting corrosion of carbon steel caused by iron bacteria. *Int Biodeterior Biodegrad* 2001;**47**:79–87. https://doi.org/10.1016/S0964-8305(99)00081-5

Sudarshan AS, Dai Z, Gabrielli M *et al*. New drinking water genome catalog identifies a globally distributed bacterial genus adapted to disinfected drinking water systems. *Environ Sci Technol* 2024;**58**:16475–87. https://doi.org/10.1021/acs.est.4c05086

Sun DL, Jiang X, Wu QL *et al*. Intragenomic heterogeneity of 16S rRNA genes causes overestimation of prokaryotic diversity. *Appl Environ Microb* 2013;**79**:5962–9. https://doi.org/10.1128/AEM.01282-13

Tsaridou C, Karabelas AJ. Drinking water standards and their implementation—a critical assessment. *Water* 2021;**13**:2918. https://doi.org/10.3390/w13202918

Viglione G. As lockdowns lift, new hazards lurk in the water. *Nature* 2020. https://doi.org/10.1038/d41586-020-01286-9

Wang H, Edwards MA, Falkinham JO *et al*. Probiotic approach to pathogen control in premise plumbing systems? A review. *Environ Sci Technol* 2013;**47**:10117–28. https://doi.org/10.1021/es402455r

Wang H, Masters S, Hong Y *et al*. Effect of disinfectant, water age, and pipe material on occurrence and persistence of *Legionella*, *Mycobacteria*, *Pseudomonas aeruginosa*, and two amoebas. *Environ Sci Technol* 2012;**46**:11566–74. https://doi.org/10.1021/es303212a

Wang Q, Garrity GM, Tiedje JM *et al*. Naive Bayesian classifier for rapid assignment of rRNA sequences into the new bacterial taxonomy. *Appl Environ Microb* 2007;**73**:5261–7. https://doi.org/10.1128/AEM.00062-07

Wang Y, Narayanan M, Shi X *et al*. Plant growth-promoting bacteria in metal-contaminated soil: current perspectives on remediation mechanisms. *Front Microbiol* 2022;**13**:966226. https://doi.org/10.3389/fmicb.2022.966226

Westcott SL, Schloss PD. OptiClust, an improved method for assigning amplicon-based sequence data to operational taxonomic units. *mSphere* 2017;**2**:e00073–17. https://doi.org/10.1128/mSphereDirect.00073-17

Whelton AJ, Dietrich AM, Gallagher DL. Contaminant diffusion, solubility, and material property differences between HDPE and PEX potable water pipes. *J Environ Eng* 2010;**136**:227–37. https://doi.org/10.1061/(ASCE)EE.1943-7870.0000147

Received 31 May 2025; **revised** 18 September 2025; **accepted** 20 September 2025